ARTICLES

Search for localized γ-ray sources along the galactic plane by an airborne experiment

R. Enomoto, J. Chiba, K. Ogawa, T. Sumiyoshi, and F. Takasaki
National Laboratory for High Energy Physics, KEK, 1-1 Oho, Tsukuba-city, Ibaraki 305, Japan

T. Kifune
Institute for Cosmic Ray Research, 3-2-1, Midori-cho, Tanashi-city, Tokyo 188, Japan

(VEGA Collaboration)

(Received 14 May 1992)

A search for localized γ-ray sources was carried out using a lead-glass-based electron telescope on board a cargo airplane. The angular resolution of this method was estimated to be 1.5 degrees, and the energy threshold was 20 GeV. Searches for γ-ray point sources along the galactic plane and for galactic diffuse γ rays were carried out. We have set the upper limits of the γ-ray intensities for various sources.

PACS number(s): 95.85.Qx, 98.70.Rz

I. INTRODUCTION

In the 1970's, two γ-ray satellites, SAS II and COS-B, observed diffuse γ-ray emissions (energy range from 100 MeV to 5 GeV) along the galactic plane and discovered approximately twenty point sources, listed in the 2CG catalogue [1]. Among them, only two (Crab pulsar and Vela pulsar) have been identified from timing correlations. Measurements with an angular resolution better than 1 deg have been necessary in order to identify those sources with objects seen via radio, optical, and x-ray observations. In the higher-energy region (from a few hundred GeV to 1 EeV), observations have been carried out by ground-based experiments with less conclusive results, except for Crab nebula [2,3]. Recently, a new γ-ray satellite [Compton Gamma Ray Observatory (CGRO)] had been launched and reported exciting results for γ-ray point sources [4]. Especially EGRET (Energetic Gamma Ray Experiment Telescope on CGRO) covers the energy range from about 20 MeV to over 20 GeV. Because of the very low flux level of the high-energy γ-rays and the limited observing period, sometimes the upper energy was lowered to 5–10 GeV [4]. In order to fill the gap between 20 GeV and 1 TeV, we have developed a new method to measure γ rays with an energy greater than 20 GeV from localized γ-ray sources.

It is quite natural to expect that γ rays in the intermediate energy range can be detected at higher altitude. Assuming a 100-GeV γ ray, it produces an electromagnetic shower cascade at higher altitude; its shower maximum is located near the airplane altitude ($\sim$10 km). By detecting one of cascade electrons, the incident γ-ray energy and its direction can be estimated. We carried out the experiments after loading the electron telescope (VEGA detector) onto a cargo airplane, and then searched for localized γ-ray sources with an energy greater than 20 GeV.

We carried out four experiments using flights between Japan and Australia during 1989 to 1991. During the first experiments in June 1989 we reported on the possibility of several point-source candidates along the galactic plane (old analysis) [5]. We briefly review these results and describe the following experimental results.

By improving the analysis method (new analysis), we could carry out a point-source search not only for the classical sources such as 2CG sources, but also for all-sky point sources and galactic diffuse γ rays.

II. EXPERIMENTAL TECHNIQUE

The depth of the secondary-electron-shower maximum induced by a γ ray is described as $T=\ln(E_0/E)-\frac{1}{2}$ r.l. (radiation length), where E_0 is the incident γ-ray energy and E is the lower limit of the secondary electron (including positron) energy. Assuming that $E_0=100$ GeV and $E=1$ GeV and $E=1$ GeV, T is 4.1 r.l., corresponding to an altitude of 13.5 km above the sea level (150 mb). At the shower maximum, the multiplicity of secondary electrons (including positrons) is given by $N_{\max}=0.066(E_0/E)$. For the above example, $N_{\max}$ becomes 6.6 [6]. The lateral spread of the shower is of an order of K/E in radius, where K is the Moliere unit; typically, a value of 20 MeV is used. Therefore, the shower spread of electrons (>1 GeV) was calculated to be 24 m at 10 km (260 mb). At the shower maximum, 95% of the particles are contained within this region. Thus, if we load a simple device of ~ 1 m^2 (which can detect secondary electron tracks) onto an airplane, the effective detection area is enlarged by a factor $N_{\max}$. The above arguments have been

verified by an EGS4 Monte Carlo simulation [7]. The energy threshold for incident γ rays by this method was calculated to be 20 GeV at $E=0.82$ GeV by a new analysis which will be described later (the threshold of the old analysis was 40 GeV at $E=1$ GeV [5]). In order to calculate the acceptance of this method, we used an EGS4 Monte Carlo analysis which included the effects of air and a detector simulation. For example, if there is a point source with an energy spectrum of $a\times(E/0.5\ \text{GeV})^{-1.2}\ \text{cm}^{-2}\text{s}^{-1}$ $(0.5<E<1000\ \text{GeV})$, the secondary electron intensity at 250 mb could be calculated to be $0.07a\ \text{cm}^{-2}\text{s}^{1}$ at a detector threshold of 0.82 GeV. Therefore, if we observe an electron intensity of $b\ \text{cm}^{-2}\text{s}^{-1}$ on the airplane, the initial γ-ray intensity at 20 GeV would be calculated to be $0.18b\ \text{cm}^{-2}\text{s}^{-1}$.

The directions of secondary electrons are disturbed by multiple Coulomb scatterings and by geomagnetic field in a unit radiation length. Both effects are of the order of 0.5 deg, and the angular difference between the secondary electrons and the incident photon becomes ~ 1 deg (1.5 deg by the new analysis and 1.2 degrees by the old one including the detector responses). These values were also derived by the EGS4 simulation.

The γ-ray sensitivity is determined by a statistical fluctuation of the background, mainly atmospheric electrons. The atmospheric electrons are produced by π^0-decayed γ rays. The π^0's are secondary products of cosmic-ray interactions with air. This intensity was precisely measured by our measurements [9]. The value was consistent with that expected from the primary cosmic-ray intensity [9]. The value was typically $3\times10^{-3}\ \text{cm}^{-2}\text{sec}^{-1}\text{sr}^{-1}$ at a 1 GeV threshold. Assuming a 14 000 cm^2 detector, 10 hours of operation, and a few $\times10^{-3}$ sr window, the minimum sensitivity (2σ) is calculated to be about $10^{-7}\ \text{cm}^{-2}\text{sec}^{-1}$ at 1 GeV at a 10 km altitude, which corresponds to a factor $\times10^{-8}\ \text{cm}^{-2}\text{sec}^{-1}$ at 20 GeV at the incidence of the air.

The airplane we used was a B747/F. Directional information was obtained from the inertial navigation system (INS). The angles of pitch, roll, and true heading were obtained with an accuracy of 0.5 deg. The accuracies of the longitude and latitude are considered to be $3+3\ T$ (T in hour) nautical miles. The altitude is obtained in terms of the outside pressure (30-feet accuracy). These data are recorded every second on a tape system called aircraft integrated data system (AIDS) with precision UT clock data. The material located above the detector is only an aluminum body, which is approximately 3-cm thick on the average. ac power (110 V, 400 Hz) was available; we used 4 kVA in total. The temperature was well controlled at around 23 ± 1 °C and the pressure was 0.7 atmosphere. We could therefore operate the detector as if it was a ground-based experiment.

The detector (VEGA detector) is shown in Fig. 1. Its main part comprises 98 modules of lead glass counters (DF6 of $120\times120\times300\text{mm}^3$) [10]. The total surface area is 1.41 m^2; the energy resolution is $4\%/\sqrt{E}$ and the stability is as good as 2%. Above the lead-glass are located four layers of plastic scintillator hodoscopes. The angular segmentation is 0.5° and the solid angle coverage is 2.03 sr. Between the hodoscopes and the lead glass, a

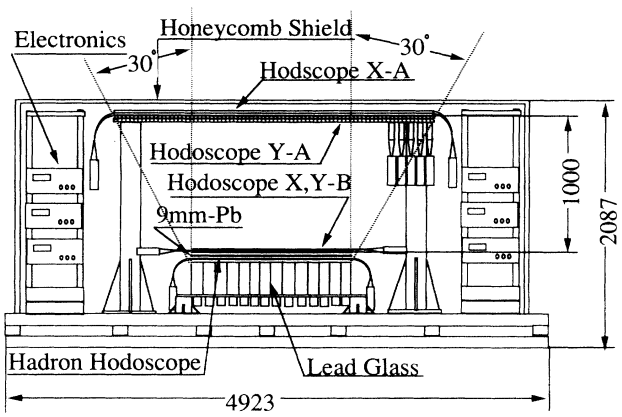

FIG. 1. Cross-sectional view of the VEGA detector.

1.5-r.l. lead sheet and a plastic scintillator hodoscope are located in order to reject hadron components. The hadron-rejection factor is as good as 20. The trigger was the coincidence of a lead-glass energy deposit and a hodoscope track. Details concerning this section is found elsewhere [8].

III. REVIEW OF THE 1989 EXPERIMENTAL RESULTS

We used a flight between Narita (Japan) and Sydney (Australia) via Guam (USA) on June 7, 1989 [Japan standard time (JST)]. The flight numbers were JL661 and JL662. In the equatorial coordinate, the detector zenith moved along the galactic plane, as shown in Fig. 2. Especially for the galactic center region, the exposure time was 3–4 hours per flight. More details can be found in Ref. [5].

The incident direction of the electrons was plotted in two-dimensional galactic coordinates. A peak search was carried out with a binning of 2 deg×2 deg. The searched region was $-30°<b<30°$, $-40°<l<80°$, where b is the galactic latitude and l is the galactic longitude. In total, there were 1800 bins. The background was made by smoothing the sideband spectra. The number of peaks obtained by a cluster-finding algorithm is plotted in Fig. 3. The figures are the b distribution of those peaks: (a), (b), and (c) were obtained by a different statistical significance cut (i.e., 1.5σ, 2.5σ, and 3.5σ). The histogram comprises experimental data and the curves Monte Carlo calculations. As can be seen from these figures, a lower significance cut gave a distribution that is consistent with the statistical fluctuation. At a higher significance cut, however, it deviated, especially for $-6°<b<6°$. We obtained eight peaks in this region, while the Monte Carlo calculation predicted 0.9 peak (we call them "galactic plane source" hereafter).

The peak positions were compared with the COS-B point sources (2CG catalogue). Peak B, which is located at $(l,b)=(358.2,+1.0)$, is close to 2CG359-00; the other peaks are far from any 2CG sources by more than 4°. The intensity of source B is $1.13\pm0.26\times10^{-7}\ \text{cm}^{-2}\text{sec}^{-1}$, assuming an integrated energy spectrum of

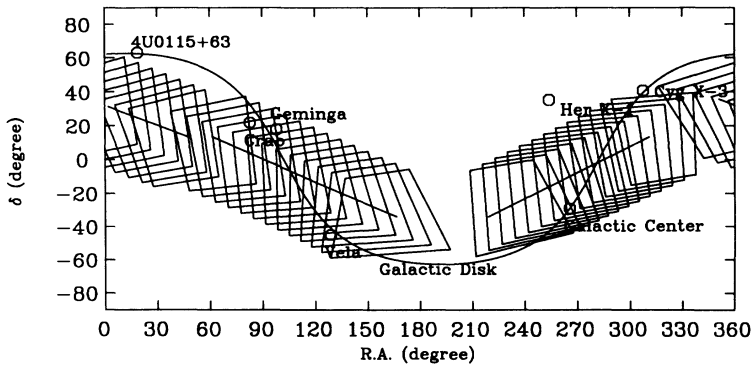

FIG. 2. Zenith positions (lines) and the field of view (squares) every 30 min for the flight JL611/662, on June 7, 1989 (JST). The curve is the galactic plane and the γ-ray point sources are indicated with circles. The coordinate is in the equatorial frame.

E^{-1}. There is a possibility that the *sources* are actually fluctuations of a broad excess from the direction of the galactic plane. Raw distributions of the electron arrival direction (l) are plotted in Fig. 4, especially inside the galactic plane and outside it.

IV. RESULTS OF 1990-1991 EXPERIMENTS

We carried out two experiments in 1990 and one in 1991 using the same flights as were used in the 1989 experiment. The dates were June 6 and 13, 1990 (JST) and June 12, 1991 (JST). In these flights we selected a higher altitude, such as 13 km above sea level (typical altitude in 1989 flight was 10 km), so as to be more sensitive to a softer energy spectrum ($E^{-\gamma}, \gamma > 1$). The experimental conditions are summarized in Table I. In total, a product of area, time, and solid angle was $2.4 \times 10^9\,\mathrm{cm^2\,s\,sr}$ at ~ 11 km above sea level. Thus, the statistics were more than triple compared to that obtained during the 1989 flight. In the 1990 flights, the dead-time counter did not work, and an additional systematic error of 10–20% should be added in the case of the γ-ray intensity measurements.

The same analysis (i.e., old analysis) was undertaken for the new data at first. However, with a 3.5σ cut we observed two, four, and one peak during the three flights, consistent with the statistical fluctuations. The results of the peak finding are plotted in Fig. 5 for three new experiments. The distributions of the electron arrival directions are plotted in Figs. 6, 7, and 8. We could not confirm the point-source results based on the 1989 experiment. In conclusion, the peaks which had been observed in the 1989 experiments might be attributed to a statistical fluctuation or the analysis bias. In order to investigate it, we carried out a new analysis to improve statistical accuracy. In addition we check the analysis biases

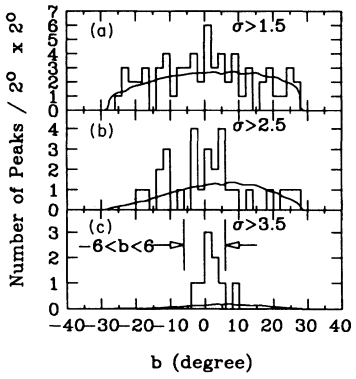

FIG. 3. Number of peaks obtained by a cluster-finding algorithm. The figures are the b distributions of those peaks: (a), (b), and (c) were obtained by a different statistical significance cut, i.e., 1.5σ, 2.5σ, and 3.5σ, respectively. Histograms were experimental data and curves were Monte Carlo calculations.

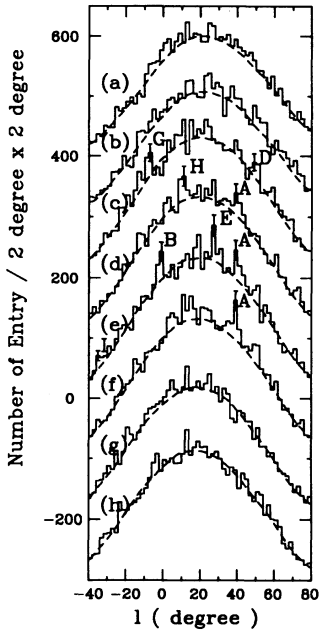

FIG. 4. Distributions of l of electrons, in the 2 degrees slices of b with vertical offset values in the parentheses: (a) $-14° < b < -12°$ (400); (b) $-12° < b < -10°$ (300); (c) $-4° < b < -2°$ (200); (d) $-2° < b < 0°$ (100); (e) $0° < b < 2°$ (0); (f) $2° < b < 4°$ (-100), (g) $10° < b < 12°$ (-200), and (h) $12° < b < 14°$ (-300). The histograms are the incident directions (l) of electrons. The dashed curves are the control backgrounds, which are made from the sideband spectra. The peaks found by the algorithm are tagged with error bars and the symbols A, B, D, E, G, H, and I. The error bars are statistical ones.

TABLE I. Summary of the experimental conditions.

Year	Date (UT)	Column density (g/cm^2)	Observation time (hours)
1989	June 7	225	7.9
1990	June 6	229	13.5
1990	June 13	227	15.0
1991	June 12	236	10.5
Total		234	46.9

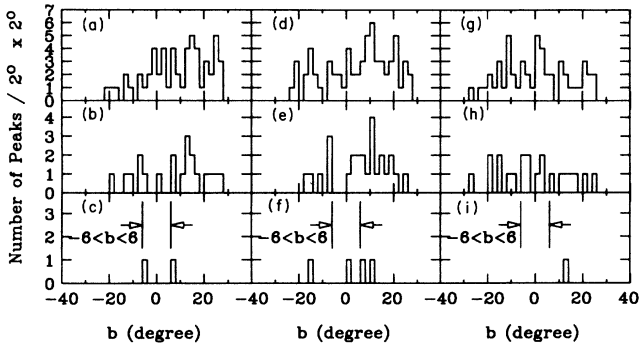

FIG. 5. Results of peak findings for new experiments. The definitions of the figures are the same as in Fig. 3

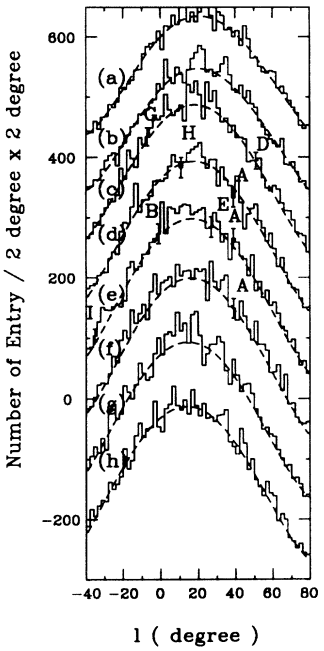

FIG. 7. Arrival directions of electrons in the June 13, 1990, experiment. The definitions of the plots are the same as in Fig. 4.

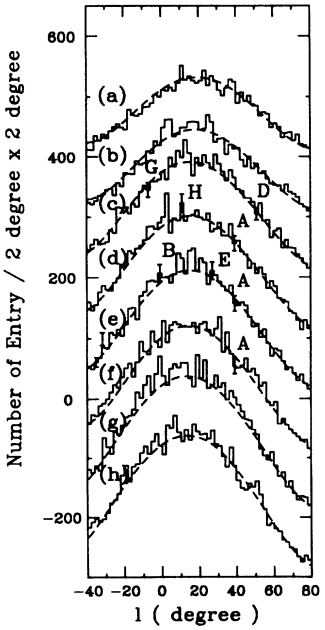

FIG. 6. Arrival directions of electrons in the June 7, 1990, experiment. The definitions of the plots are the same as in Fig. 4.

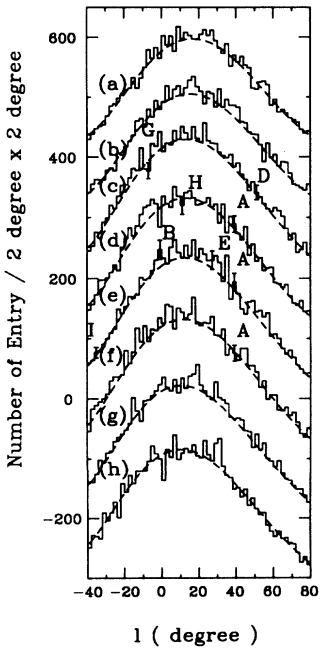

FIG. 8. Arrival directions of electrons in the June 12, 1991, experiment. The definitions of the plots are the same as in Fig. 4.

TABLE II. Observed integrated intensities at 40 GeV for the galactic phase sources in the 1989 analysis are shown. The peak identification (peak ID) was the same as described in Ref. [5].

Peak (ID)	Position l,b (deg)	$I(\gamma=1,1989)$ 10^{-7} cm^{-2}s^{-1}
A	39.4, +2.1	1.13±0.26
B	358.2, +1.0	0.64±0.17
C	32.8, +1.0	0.80±0.23
D	50.2, +2.1	0.98±0.29
E	27.1, +0.5	0.71±0.22
F	4.0, +9.0	0.53±0.17
G	352.4, −3.0	0.50±0.17
H	10.1, −1.0	0.45±0.15
I	325.4, +1.0	0.49±0.19

carefully using Monte Carlo methods. The upper limits of the γ-ray intensities for these peaks were obtained using an improved analysis method (new analysis), which is discussed in the next section.

V. NEW ANALYSIS

In order to obtain upper limits of the γ-ray intensity for the galactic plane γ-ray sources reported in 1989 [5], we developed an improved analysis. The differences from the old analysis are as follows.

(1) The threshold energy was minimized to the hardware threshold. The average hardware threshold was measured to be 820 MeV. This improved the γ-ray sensitivity about by 10–20%, depending on the energy spectrum. The loss in the angular resolution was only 10%.

(2) Sometimes there was a lack of INS data for a few minutes or so. However considering the motion of the aircraft, a deterioration of the angular resolution was quite small ($\ll 1°$). In these cases we applied the interpolation of the INS data. We also monitored subsecond airplane motion by a clinometer sensor. There was no big disturbance of more than 1° within several hours of flight.

(3) In the old analysis, we used a cut on the number of hodoscope hits in order to avoid any directional ambiguity. According to the detailed EGS4 simulation, however, since these effects could be fully understood, we removed this cut.

This improved the electron acceptances much greater than by a factor of 2. In total, the gain of the acceptance was about three. The threshold energy at the γ-ray incidence was lowered from 40 to 20 GeV. The angular resolution of this analysis was 1.5±0.1 degrees. Since the angular resolution of the old analysis was 1.2±0.1 degrees, the gain for the γ-ray sensitivity was improved by a factor of 1.5 or more for each experiment. We also added all of the experimental data and searched for peaks.

Based on the above-mentioned analysis method, we derived upper limits for the galactic plane γ-ray sources. Table II is a summary obtained by the 1989 analysis used for a comparison. The γ-ray energy spectrum was assumed to be E^{-1}; no cutoff energy was assumed in these values. However, it is quite natural to set a high-energy cutoff in the energy spectrum. Because the ground-based experiments are sensitive to an energy greater than 1 TeV, in the new simulation we set a 1-TeV cutoff in the γ-ray energy spectrum. Thus, these values given in Table II are considered somewhat overestimated. By applying a 1-TeV cutoff in the initial γ-ray spectrum (in this case the spectrum of E^{-1} was assumed), an attenuation factor by a 250-mb air was calculated to be increased by a factor of 2.1 compared to the case without upper energetic cutoff. Thus in order to compare the new upper limits at 20 GeV with the old values at 40 GeV in Table II, a factor of 4.2($=2.1\times2$) must be multiplied to the old values.

The fitting was carried out in 2σ slices in b of a two-dimensional (l versus b) plot of the electron arrival direction. All of the available data were used. The fitting function was a sixth-order polynomial plus a Gaussian with a point spread function. In the scanning we could not observe any statistically significant peaks. The 90% confidence level (C.L.) upper limits for integrated γ-ray intensities at 20 GeV are summarized in Table III. The upper limits were obtained assuming various energy spectra of $E^{-\gamma}$ with a cutoff energy of 1 TeV. The systematic uncertainty for the integrated intensity was considered to be less than 20%; this value was included in the upper limits.

The peaks still remained in a new analysis for the 1989 dataset; however, the statistical significances of these peaks decreased. There was a suggestion that they come from the material distribution of the airplane ceiling; in

TABLE III. 90% C.L. upper limits (UL's) for the integrated intensities of galactic plane γ-ray sources at 20 GeV. The peak identification (peak ID) was the same as described in Ref. [5].

Peak ID	UL($\gamma=1$) 10^{-8} cm^{-2} s^{-1}	UL($\gamma=1.2$) 10^{-8} cm^{-2}s^{-1}	UL($\gamma=1.4$) 10^{-8} cm^{-2}s^{-1}	UL($\gamma=1.6$) 10^{-8} cm^{-2}s^{-1}	UL($\gamma=1.8$) 10^{-8} cm^{-2}s^{-1}
A	8.3	8.3	7.9	8.0	7.0
B	8.0	8.4	8.6	9.9	9.7
C	13.6	13.6	12.9	13.2	11.5
D	10.2	10.3	9.8	10.1	8.8
E	8.8	8.9	8.5	8.7	7.7
F	10.6	11.0	11.1	12.5	12.1
G	8.7	9.2	9.6	11.2	11.3
H	17.6	18.2	17.9	19.5	18.1
I	30.2	32.9	37.1	39.9	36.6

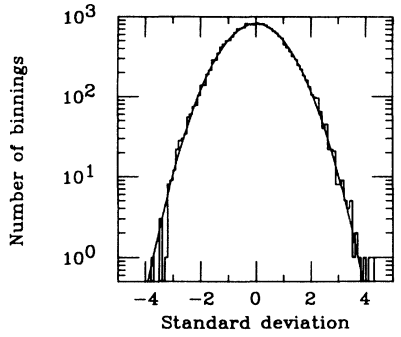

FIG. 9. Distribution of the standard deviations for the peak entry by the new fitting procedure described in the text. The histogram is the raw data, and the curve is the best-fitted Gaussian function.

the airplane frame, however, no positional correlations were obtained. In conclusion, the peaks that had been observed in the 1989 experiments might be attributed to a a statistical fluctuation.

VI. γ-RAY POINT SOURCE SEARCH

We carried out an all-sky peak search using all of the available data. The region was defined so that the entry inside the binning had more than 20% of the peak entry. The bin size was reduced to 1 deg$\times$1 deg; in total there were 21 015 binnings. Peak fitting was carried out in a one-dimensional slice ($|b-b_0|<3$ deg(2σ), $|l-l_0|<30$ deg), where b_0 and l_0 were the positions of the target binnings. A 6th-order polynomial function plus a Gaussian was used. In total, five fittings were performed every 0.2-deg l step in each target binning, and the upper limits were calculated from the maximum peak entry obtained by these five procedures. The b_0's and l_0's were varied by a 1 deg step.

The distribution of the standard deviations for the fitted peak entry is shown in Fig. 9. The standard deviation was defined as being the peak entry divided by its error. The distribution was consistent with the normal distribution. The best-fitted Gaussian shows a center position of $-8\pm7\times10^{-3}$ and a width of 1.010±0.005. There were no significant deviations in the higher standard deviations. We plotted the b positions of the peaks using the various standard deviation cuts (1.5σ, 2.5σ, and 3.5σ) in Fig. 10. The distributions were scaled with the number of binnings; we could not see any statistically significant deviations in the higher σ cut. Although there were seven binnings obtained by a 3.5σ cut, six of them came from the same peak at around $(l,b)=(-107$ deg, 23 deg). The statistical significance of the peak was 4.2σ (C.L.$=3\times10^{-5}$). By multiplying the number of binnings, the probability of a chance coincidence was calculated to be 60%. We thus concluded that there were no significant peaks within the entire region. Once again we

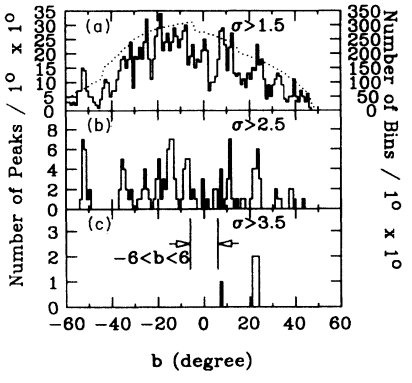

FIG. 10. The b distributions of the peaks obtained by the new analysis using three different standard deviation cuts: (a) 1.5σ cut, (b) 2.5σ cut, and (c) 3.5σ cut. For reference, the b projection of the number of binnings (right scale) is overdrawn by the dotted curve in (a).

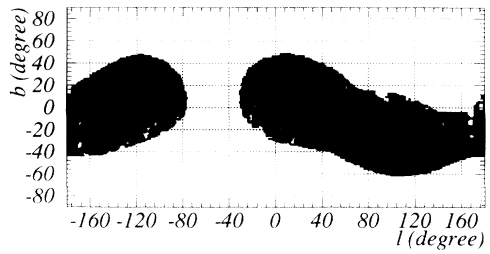

FIG. 11. Region where there were no γ-ray point sources with integrated intensities with more than 3×10^{-7} cm^{-2}s^{-1} at 20 GeV.

TABLE IV. 90% C.L. upper limits for the integrated intensities of 2CG sources at 20 GeV. Also shown are fluxes of the extrapolation at 20 GeV using COS-B data. The energy spectra of E^{-1} was used.

Source name	Upper limits 10^{-7} cm^{-2}s^{-1}	Extrapolation at 20 GeV (COS-B) 10^{-7} cm^{-2}s^{-1}
2CG006−00	0.90	0.12
2CG010−31	2.53	0.06
2CG013+00	1.11	0.05
2CG036+01	0.86	0.10
2CG054+01	1.23	0.07
2CG065+00	1.96	0.06
2CG075+00	1.16	0.07
2CG078+01	1.19	0.13
2CG095+04	2.81	0.06
2CG121+04	1.96	0.05
2CG184−05	2.50	0.19
2CG195+04	1.80	0.24
2CG218−00	1.59	0.05
2CG235−01	0.93	0.05
2CG263−02	2.36	0.66
2CG333+01	1.71	0.19
2CG342−02	1.86	0.10
2CG353+16	0.95	0.06
2CG356+00	1.28	0.13
2CG359−00	1.36	0.09

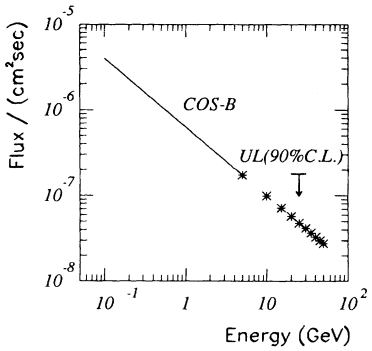

FIG. 12. Upper limit of γ-ray integrated intensities above 20 GeV for Geminga. The solid line is COS-B observation and the asterisks are the extrapolations of the COS-B energy spectrum.

could not confirm the results obtained by the 1989 experiment. There was no significant excess around the galactic plane.

By the above-mentioned fitting procedure we obtained the 90% C.L. upper limits for the γ-ray point sources at 20 GeV in the entire searched region. Since there was no big spectrum dependence in the upper-limits estimation, as shown in Table III, the energy spectrum was assumed to be proportional to $E^{-1.2}$, and a cutoff energy of 1 TeV was assumed. The region where there were no intense point sources with integrated intensities greater than 3×10^{-7} cm^{-2}s^{-1} is shown in Fig. 11. Most of the region was rejected due to the above hypothesis.

VII. UPPER LIMITS FOR 2CG SOURCES

Using the upper limits obtained by the above-mentioned procedures, we could set upper limits for several 2CG sources [1]. Unfortunately the very strong γ-ray quasar 3C279 which had been observed by CGRO was outside our sensitive celestial range [4]. The 90%-CL upper limits are summarized in Table IV. Values of around 10^{-7} cm^{-2}s^{-1} were typical for these sources. Especially for Geminga (2CG195+0.4), our upper limit is shown in Fig. 12 with the extrapolated intensities calculated from the COS-B data [12]. In order to detect positive results for some of these sources, we need 10 times more sensitivity. This could be realized by the following improvements: (1) 10 times more surface area (15 m^2=2.5 m$\times$6 m, i.e., 2 slots in B747/F); (2) add γ-ray detection with directional measurements (gain >2); (3) more flights ($\sim$5 times). These parameters can be realized by using a scintillating fiber calorimeter with an image intensifier readout or a multianode phototube readout.

VIII. SEARCH FOR GALACTIC DIFFUSE γ RAY

In the case of the ground-based experiments, the background for galactic diffuse γ rays is cosmic-ray nucleons. The typical signal-to-noise (S/N) ratio is considered to be 10^{-5}. In our case, the background is the secondary electrons initiated by the primary cosmic-ray nucleons. The galactic diffuse γ ray is considered to be produced by the same mechanism as the atmospheric electrons. The difference is whether the target is interstellar matter or air. The signal-to-noise ratio is considered the same as the ratio of the material thickness for these two; the expected S/N ratio in our case is 10^{-3}. Therefore, our sensitivity for galactic diffuse γ rays is of the same order, or better, compared to the ground-based experiments. Also, since the VEGA detector has a large solid angle ($\sim$1 sr), background subtraction is much easier than that by the air Cherenkov experiments.

The COS-B experiment observed different energy spectra between the inner galaxy ($|l|<50°$) and the outer galaxy ($|l-180°|<90°$), as shown in Fig. 13. At a maximum energy of 6 GeV, their intensities coincide. The ratio of these two intensities suggested that there was a difference of $\sim$0.4 in the power spectrum of $E^{-\gamma}$ [12]. If this is correct, the γ-ray intensity of the outer galaxy became stronger than that of the inner galaxy at a 10-GeV region; there appears to be a possibility of detection by our measurement. Our measurement might give a constraint to models such as outer galaxy cosmic-ray acceleration or the inversed Compton scattering.

The search was carried out using b projections of the arrival directions of electrons in a specific l range. We used the same l range as that by the COS-B experiment. The fitting function was a seventh-order polynomial plus a Gaussian. The width of the Gaussian was assumed to be $\sqrt{3.5^2+1.5^2}$ deg in b, where 3.5 deg was the width observed for galactic diffuse γ rays at the GeV region by SAS II and COS-B; 1.5 deg was our point spread function. The peak position was varied in $|b|<3°$ by 0.2-deg step.

The results are shown in Figs. 14(a)–14(c), for inner, outer galaxy and total sensitive region, respectively. There were unknown structures, however, that were outside of the fitting range, i.e., $|b|>3°$. Therefore, we set the 3σ upper limits for the galactic diffuse γ ray intensi-

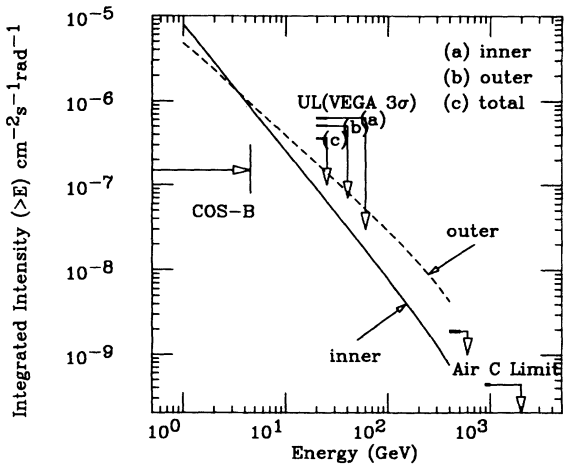

FIG. 13. Upper limits of the integrated intensity of the galactic diffuse γ ray at 20 GeV: (a) for inner galaxy, (b) for outer galaxy, and (c) for the total region. The curves are the extrapolated intensity by the COS-B experiment. The limits obtained by the air Cherenkov experiments are also shown.

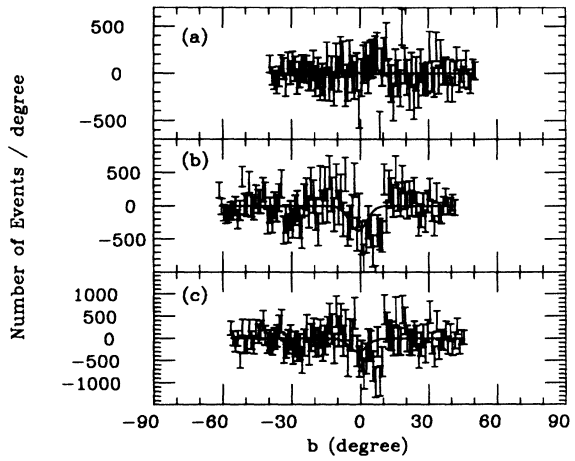

FIG. 14. The b projection of the background-subtracted arrival directions of electrons: (a) for $|l|<50°$, (b) for $|l-180°|<90°$, and (c) for all region.

ties; the values are given in Fig. 13. The acceptance was calculated using the energy spectrum of the COS-B data and its extrapolation ($E^{-\gamma}$ for the inner galaxy and $E^{\gamma-0.4}$ for the outer galaxy). Although the values were obtained using $\gamma=1.5$, there were no big differences when γ was changed from 1.5 to 1.8.

The upper limits were 6.3×10^{-7}, 5.1×10^{-7}, and 3.6×10^{-7} cm^{-2}s^{-1} rad^{-1}, for the inner, outer galaxy, and total region, respectively. They are slightly larger than the COS-B extrapolated values of 1.8×10^{-7} cm^{-2}s^{-1} rad^{-1}. We could therefore not reject the hypothesis of cosmic-ray accerlation in the outer galaxy. If we assumed COS-B extrapolation in the inner galaxy, we could set an upper limit in the power spectrum difference between the outer and inner galaxy; its value was 0.90 (3σ) in the 6–20 GeV energy range. We could also set an upper limit of the integrated energy spectrum power index of the outer galaxy to be more than 0.60 (3σ) in the 6–1000 GeV energy range. In addition, we derived the upper limits of the signal-to-atmospheric-electron-intensity ratio to be 4.3×10^{-3}, 3.3×10^{-3}, and 2.4×10^{-3}, for the inner, outer galaxy, and total region, respectively. This suggested that the interstellar material with which cosmic rays interact was less than an order of 0.24 gram.

The limits obtained by the air Cherenkov experiments are also shown in Fig. 13 [13]. Comparing the upper limits to the fluxes of inner galactic diffuse γ rays, the sensitivity of our experiment was found to be the same order to that of air Cherenkov experiments. In the case of ours, by improving the detector sensitivity by a factor of 10, a positive measurement will be possible.

IX. CONCLUSION

We searched for localized γ-ray sources at energies greater than 20 GeV over a wide celestial region. We loaded a lead-glass-based electron telescope onto the cargo airplane and measured the energy and direction of secondary electrons. Typical sensitivities for point sources and galactic diffuse γ rays were 10^{-7} cm^{-2}s^{-1}, and 1×10^{-7} cm^{-2}s^{-1}rad^{-1} at 20 GeV, respectively; the angular resolution was 1.5 degrees. We carried out four flights in total from 1989 to 1991. The searched region was around the galactic plane.

In the 1989 experiments we had observed several point-source candidates along the galactic plane. However, in three out of four experiments, since these source were not confirmed, we set their upper limits. Also the upper limits of point sources within a wide celestial region and galactic diffuse γ ray were set.

ACKNOWLEDGMENTS

We appreciate support from Professor J. Nishimura (Institute for Space and Astronautical Science), Professor H. Sugawara, Professor K. Kikuchi, Professor K. Takahashi, Professor S. Iwata, Professor M. Kobayashi, Mr. Y. Ukita (KEK), Professor J. Arafune (ICRR), Dr. Y. Takahashi (University of Alabama), Professor T. Kamae, and Dr. T. Takahashi (University of Tokyo) in proceeding with this plan. This work was partially supported by a Grant-in-Aid for Scientific Research on Priority Areas from the Japan Ministry of Education, Science, and Culture. We thank T. Hakamada of Hamamatsu Photonics K. K. for cooperation. Finally, we deeply appreciate M. Iizuka (Japan Airlines Co., Ltd.) for his substantial help and cooperation.

[1] G. F. Bignami and W. Hermsen, Annu. Rev. Astron. Astrophys. **21**, 67 (1983); H. A. Mayer-Hasselwander and G. Simpson, in *Proceedings of the Twenty-First International Cosmic Ray Conference,* Adelaide, Australia, 1989, edited by R. J. Protheroe (Graphic Services, Northfield, 1990), Vol. 1, p. 261.

[2] R. C. Lamb, in *Relativistic Astrophysics,* Proceedings of the Thirteenth Texas Symposium, Chicago, Illinois, 1986, edited by M. P. Ulmer (World Scientific, Singapore, 1987), p. 589.

[3] G. Vacanti *et al.*, Astrophys. J. **377**, 469 (1991).

[4] R. C. Hartman *et al.*, Astrophys. J. **385**, L1 (1982); B. L. Bertsch *et al.*, Nature **357**, 306 (1992).

[5] R. Enomoto *et al.*, Phys. Rev. Lett. **64**, 2603 (1990).

[6] J. Nishimura, in *Hand Book der Physik,* edited by S. Flügge and K. Sette (Springer, Verlag, Berlin, 1967), Vol. 46, p. 1.

[7] W. R. Nelson *et al.*, Report SLAC-265, 1985 (unpublished).

[8] R. Enomoto *et al.*, Nucl. Instrum. Methods **A295**, 261 (1990).

[9] R. Enomoto *et al.*, Phys. Rev. D **44**, 3419 (1991).

[10] K. Ogawa *et al.*, Nucl. Instrum. Methods **A243**, 58 (1986); T. Sumiyoshi *et al.*, *ibid.* **A271**, 432 (1988).

[11] J. L. Masnou *et al.*, in *Proceedings of the 17th International Cosmic Ray Conference,* Paris, France, 1981 (CEN, Sa-

clay, 1981), Vol. 1, p. 177.
[12] J. B. G. M. Bloemen, Astrophys. J. **317**, L15 (1987).
[13] P. T. Reynolds *et al.*, in *Proceedings of the 21th International Cosmic-Ray Conference,* [1], Vol. 2, p. 383; C. W. *et al.*, in *Proceedings of the 22nd International Cosmic Ray Conference,* Dublin, Ireland, 1991, edited by M. Cawley *et al.* (Dublin Institute for Advanced Studies, Dublin, 1992).

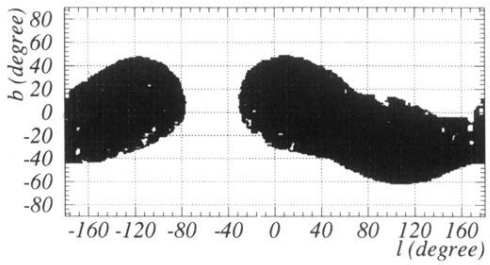

FIG. 11. Region where there were no γ-ray point sources with integrated intensities with more than 3×10^{-7} cm^{-2}s^{-1} at 20 GeV.